THE JOURNAL OF BIOLOGICAL CHEMISTRY VOL. 284, NO. 51, pp. 35839–35849, December 18, 2009


# Cardiac-specific Deletion of LKB1 Leads to Hypertrophy and Dysfunction[S]

Received for publication, September 1, 2009, and in revised form, October 7, 2009 Published, JBC Papers in Press, October 14, 2009, DOI 10.1074/jbc.M109.057273

**Yasumasa Ikeda[‡1], Kaori Sato[‡], David R. Pimentel[§], Flora Sam[¶2], Reuben J. Shaw[‖], Jason R. B. Dyck[**3], and Kenneth Walsh[‡4]**

*From the [‡]Molecular Cardiology/Whitaker Cardiovascular Institute, Boston University School of Medicine, the [§]Cardiovascular Medicine Section, Department of Medicine, Boston University Medical Center and Myocardial Biology Unit, Boston University School of Medicine, and the [¶]Cardiac Remodeling Laboratory/Whitaker Cardiovascular Institute, Boston University School of Medicine, Boston, Massachusetts 02118, the [‖]Molecular and Cell Biology Laboratory, Salk Institute for Biological Studies, San Diego, California 92186, and the **Cardiovascular Research Centre, University of Alberta, Edmonton, Alberta T6G 2S2, Canada*

**LKB1 encodes a serine/threonine kinase, which functions upstream of the AMP-activated protein kinase (AMPK) superfamily. To clarify the role of LKB1 in heart, we generated and characterized cardiac myocyte-specific LKB1 knock-out (KO) mice using α-myosin heavy chain-Cre deletor strain. LKB1-KO mice displayed biatrial enlargement with atrial fibrillation and cardiac dysfunction at 4 weeks of age. Left ventricular hypertrophy was observed in LKB1-KO mice at 12 weeks but not 4 weeks of age. Collagen I and III mRNA expression was elevated in atria at 4 weeks, and atrial fibrosis was seen at 12 weeks. LKB1-KO mice displayed cardiac dysfunction and atrial fibrillation and died within 6 months of age. Indicative of a prohypertrophic environment, the phosphorylation of AMPK and eEF2 was reduced, whereas mammalian target of rapamycin (mTOR) phosphorylation and p70S6 kinase phosphorylation were increased in both the atria and ventricles of LKB1-deficient mice. Consistent with vascular endothelial growth factor mRNA and protein levels being significantly reduced in LKB1-KO mice, these mice also exhibited a reduction in capillary density of both atria and ventricles. In cultured cardiac myocytes, LKB1 silencing induced hypertrophy, which was ameliorated by the expression of a constitutively active form AMPK or by treatment with the inhibitor of mTOR, rapamycin. These findings indicate that LKB1 signaling in cardiac myocytes is essential for normal development of the atria and ventricles. Cardiac hypertrophy and dysfunction in LKB1-deficient hearts are associated with alterations in AMPK and mTOR/p70S6 kinase/eEF2 signaling and with a reduction in vascular endothelial growth factor expression and vessel rarefaction.**

LKB1 is a ubiquitously expressed serine/threonine kinase that functions upstream of the 13 members of the AMP-activated protein kinase (AMPK)[5] superfamily (1). Analyses of LKB1-knock-out (KO) mouse models reveal that this kinase controls the physiological functions of many tissues. For instance, whole body LKB1-KO mice display embryonic lethality due to defects in the development of the neural tube, mesenchymal cell death, and abnormal vascular development (2). In addition, tissue-specific ablation of LKB1 has revealed that LKB1 also plays a major role in the regulation of cellular metabolism, likely via its role as an upstream AMPK-kinase (3–5). Although the role of LKB1 in the regulation of metabolic processes is under intense investigation, LKB1 also functions as a tumor suppressor, and its loss leads to the development of Peutz-Jeghers syndrome (6, 7). Importantly, at a cellular level LKB1 controls proliferation and cell polarity (8), which contributes to the tumor-inhibitory actions of LKB1.

Consistent with the role of LKB1 in cell growth control, our recent work has shown that increased cardiac myocyte LKB1 activity contributes to the inhibition of protein synthesis involved in cardiac hypertrophy (9). Conversely, reduced LKB1 expression and/or activity has been shown in the hypertrophied hearts of various transgenic mouse models (9, 10), suggesting that pathological inhibition of LKB1 activity may be an important contributor to the hypertrophic process. In agreement with this, oxidative stress-mediated inhibition of LKB1 in hypertensive rats also appears to promote prohypertrophic signaling (11). However, despite the potential importance of LKB1 activity in terms of regulating cardiac hypertrophy, very few studies have specifically investigated LKB1 signaling in the heart and its role in atrial and ventricular development and remodeling.

Previously, Sakamoto *et al.* (12) characterized the cardiac phenotype of mice using a MCK-Cre deletor strain that is expressed primarily in skeletal muscle and secondarily in cardiac muscle. They reported that these mice develop biatrial enlargement and reduced ventricular size while maintaining

[S] The on-line version of this article (available at http://www.jbc.org) contains supplemental Fig. 1 and Table 1.

[1] Supported by the Japan Health Sciences Foundation.
[2] Supported by National Institutes of Health Grant HL079099.
[3] Alberta Heritage Foundation for Medical Research Senior Scholar and a Canada Research Chair in Molecular Biology of Heart Disease and Metabolism and supported by Canadian Institutes of Health Research Grant MOP53088.
[4] Supported by National Institutes of Health Grants HL68758, HL77774, HL86785, and AG15052. To whom correspondence should be addressed: Molecular Cardiology/Whitaker Cardiovascular Institute, Boston University Medical Campus, 715 Albany St., Rm. W611, Boston, MA 02118. Tel.: 617-414-2390; Fax: 617-414-2391; E-mail: kxwalsh@bu.edu.

[5] The abbreviations used are: AMPK, AMP-activated protein kinase; ACC, phosphoacetyl-CoA carboxylase 1; Ad, adenovirus; Afib, atrial fibrillation; caAMPK, constitutively active AMPK; CREB, cAMP-responsive-binding protein; DCREB, constitutively active CREB; dP/dt, first derivative of left ventricular pressure; KO, knock-out; SERCA, sarcoendoplasmic reticulum $Ca^{2+}$-ATPase; MHC, myosin heavy chain; mTOR, mammalian target of rapamycin; siRNA, small interfering RNA; VEGF, vascular endothelial growth factor; MCK, muscle creatine kinase.

normal cardiac systolic function. However, the MCK-Cre strain used by Sakamoto *et al.* (12) does not efficiently delete genes in heart (13, 14). Furthermore, the systemic consequences of LKB1 ablation in skeletal muscle of this strain could conceivably confound the cardiac phenotype especially given the fact that muscle fuel metabolism is altered in these mice (4). Because the role of LKB1 in the cardiac myocyte has been shown to involve the regulation of signaling molecules involved in protein synthesis and cell growth (9) as well as oxidative stress-induced hypertrophy (15), we explored the importance of LKB1 in controlling these prohypertrophic pathways by generating cardiac-specific LKB1 knock-out mice by crossing $LKB1^{flox/flox}$ mice with the $\alpha$-myosin heavy chain ($\alpha$-MHC)-Cre deletor strain. We also performed a series of LKB1 knockdown studies in cultured cardiac myocytes to understand better the functional consequences of LKB1 deficiency and the regulatory links with downstream signaling steps.

## EXPERIMENTAL PROCEDURES

*Animal Preparation and Tissue Harvest*—Cardiac myocyte-specific LKB1-deficient mice were generated by crossing $LKB1^{flox/flox}$ mice (16) with transgenic mice expressing Cre-recombinase from the $\alpha$-MHC promoter. At the indicated time points, mice were anesthetized, and excised hearts were separated into atria and ventricle. The weights of atria and ventricles were recorded, and tissues were frozen in liquid nitrogen for subsequent molecular analysis, respectively. The Institutional Animal Care and Use Committee at Boston University approved all animal studies.

*Echocardiography*—Transthoracic echocardiography was performed using a Vevo770 High Resolution Imaging System with 30-MHz RMV-707B scanning head (VisualSonics, Inc., Toronto, Ontario, Canada). Mice were anesthetized with ~2% isoflurane inhalation, and the heart rates were kept at 450–500 beats/min. The left atrium was detected in the parasternal long axis view at the aortic root and measured in the systole phase at its maximal dimension during M-mode images. The methods of measurements in left ventricular dimension and left ventricular fractional shortening (%FS) calculation were described previously (17).

*Invasive Cardiac Hemodynamic Analysis*—Hemodynamic analysis was performed with a 1.4F catheter tip micromanometer (ARIA; Millar Instruments, Houston, TX) to determine maximum systolic pressure, left ventricular end-diastolic pressure, and the first derivative of left ventricular pressure (dP/dt) by Power Lab SP Software (Ad Instruments) as described previously (18). Heart rate was maintained at 450–500 beats/min during the procedure.

*cDNA Synthesis and Quantitative Real Time PCR*—Atria and ventricular tissue were homogenized in TRIzol reagent, and RNA was extracted as described previously (17). A QuantiTect Reverse Transcription kit (Qiagen, Valencia, CA) was used to synthesize cDNA, and PCR was performed using the iCycler iQ Real Time PCR Detection Systems (Bio-Rad) with SYBR Green dye (19). Transcript levels were adjusted relative to the expression of 36B4 (20). The sequences of PCR primer are noted in supplemental Table 1.

*Western Blot Analysis*—Atrial and ventricular tissue were homogenized in T-PER reagent (Pierce) with a protease inhibitor mixture (Roche Applied Science) as described previously (17). Immunoreactive bands were visualized using ECL or ECL-PLUS chemiluminescence reagent (Amersham Biosciences) treatment and exposure to Hyperfilm-ECL. ImageJ 1.31 software was used for the quantification of the band density. Antibodies against phospho-Akt ($Ser^{473}$), total Akt, phospho-AMPK$\alpha$ ($Thr^{172}$), total AMPK$\alpha$, phosphoeukaryotic translation elongation factor 2 (eEF2) ($Thr^{56}$), total eEF2, phospho-CREB ($Ser^{133}$) total CREB, phospho-mTOR ($Ser^{2448}$), phospho-mTOR ($Ser^{2481}$, total-mTOR, phospho-p70S6 kinase ($Thr^{389}$), and total p70S6 kinase were from Cell Signaling Technology (Beverly, MA). Antibodies against Connexin 40 and 43, sarcoendoplasmic reticulum $Ca^{2+}$-ATPase (SERCA) 2A and VEGF were from Santa Cruz Biotechnology, Inc. (Santa Cruz, CA). Other antibodies used were phospholamban (Thermo Fisher Scientific), Connexin 45 (Zymed Laboratories Inc. (Invitrogen), phosphoacetyl-CoA carboxylase 1 (ACC) ($Ser^{79}$), and total ACC (both from Millipore (Upstate), Billerica, MA). The antibody against $\alpha$-tubulin (Calbiochem) was used as a loading control. Each lane was loaded for equal protein. The relative change in protein phosphorylation was calculated from the ratio of phosphorylation to total protein.

*Histological Analysis*—Whole hearts were excised and placed overnight in 10% neutral buffered formalin. After fixation, samples were embedded in paraffin, cut into 6-$\mu$m sections, and then stained with Masson's trichrome (Sigma-Aldrich). The diameters of left atrial and left ventricular myocytes were measured. The diameter was measured at the longitudinal line of the myocyte nucleus. Approximately 100 cells were measured in each section using ImageJ 1.31 software. To determine capillary density, atria and ventricles were embedded in OCT compound (Sakura Finetech USA, Inc., Torrance, CA) and snap frozen in liquid nitrogen. Cryosections (5 $\mu$m) were fixed with 4% paraformaldehyde and stained with anti-CD31 (BD Pharmingen), and hematoxylin was used for counterstaining. Capillary density was assessed in 10 randomly selected power fields.

*Cultured Neonatal Rat Cardiac Myocytes*—Primary neonatal rat cardiac myocytes were isolated and cultured as described previously (21). Cells were incubated with serum-free medium for 24 h prior to each experiment. The siRNA for LKB1 and nontargeting control were purchased from Dharmacon (siGENOME SMART Pool and ON-TARGETplus siCONTROL NonTargeting siRNA Pool) and used as reported previously (19). Cells were infected with adenovirus constructs encoding constitutive active form AMPK$\alpha$1(Ad-caAMPK) (22) or $\beta$-galactosidase at a multiplicity of infection of 50 for 24 h. RNA and protein extractions from cardiac myocytes were described previously (19). The adenoviral vector expressing a constitutively active form of CREB (Ad-DCREB) was a gift from Dr. Reusch (University of Colorado Health Sciences Center). For the assessment of hypertrophy, cardiac myocytes were plated on chamber slide (LAB-TEK II Chamber slide, Thermo Fisher Scientific). Cells were fixed with 4% paraformaldehyde for 10 min and stained with anti-$\alpha$-actinin (Sigma-Aldrich) overnight at 4 °C to visualize sarcomere structure. Cell surface area was measured from at least 100 cardiac myocytes/well in four independent experiments using ImageJ software. For analysis of protein synthesis, cardiac myocytes were plated in 24-well plates, and [$^3$H]leucine incorporation was measured (23). After each treatment, [$^3$H]leucine (1 $\mu$Ci/ml) was added, and cells

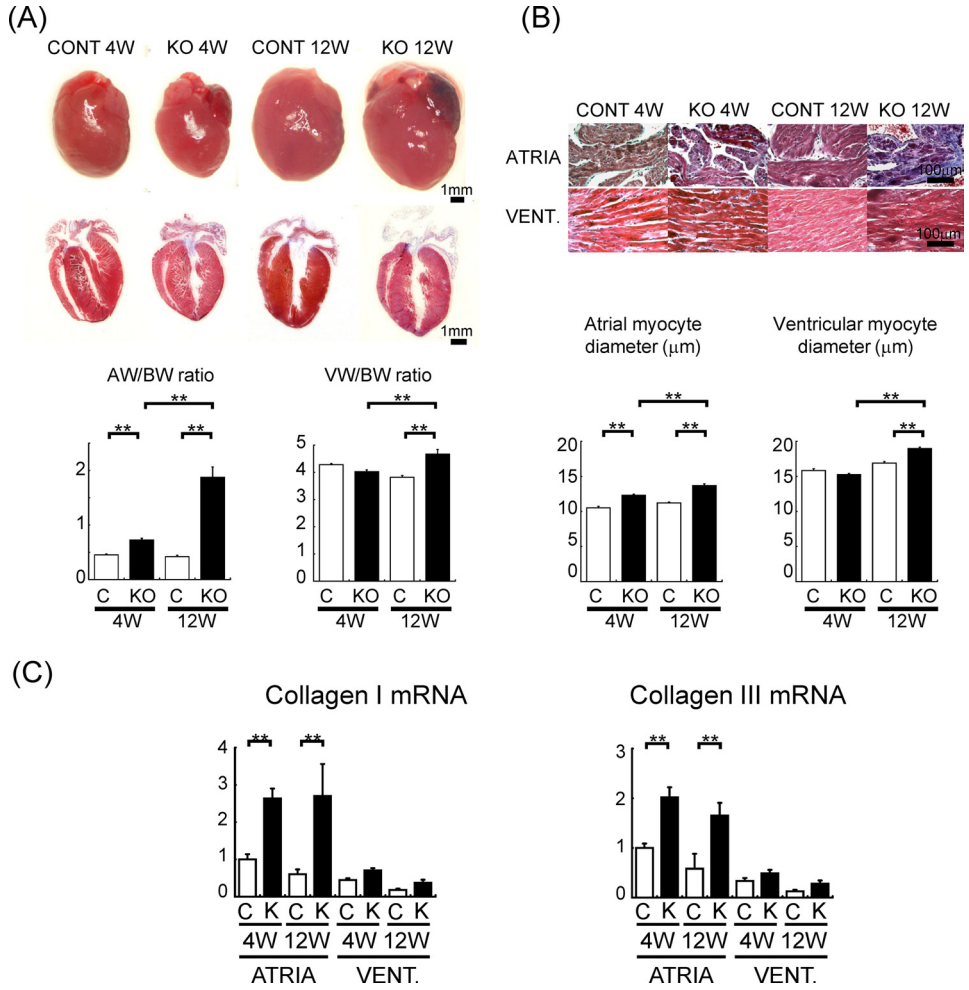


FIGURE 1. **Analysis of the cardiac phenotype in control and LKB1-KO mice at 4 and 12 weeks of age.** *A*, gross appearance of the isolated hearts (*top*) and long axis section of four-chamber view with Masson's trichrome staining (*middle*). The mean atrial and ventricular weight to body weight ratios are also shown (*bottom*). *B*, histological sections of Masson's trichrome-stained left atrial and left ventricular tissue (*upper*). The mean atrial and ventricular myofibrillar transverse diameter in control (*open bars*) and LKB1-KO (*filled bars*) mice (*lower*) are shown. Values are expressed as mean ± S.E. **, $p < 0.01$; each group $n = 5–7$. *C*, mRNA level of collagen I and III expression in atria and ventricles of control and LKB1-KO mice. The real time PCR analyses were performed in control (*open bars*) and LKB1-KO (*filled bars*) at 4 and 12 weeks of age, respectively. Values are change relative to each control band (4-week-old control atria) and are expressed as mean ± S.E. **, $p < 0.01$; $n = 6$ in each group.

were incubated for an additional 4 h. Cells were washed three times with 1× PBS and incubated with 10% trichloroacetic acid for 30 min at 4 °C to prepare precipitated proteins. The precipitated material was washed three times with 1× PBS and then neutralized with 0.5 N NaOH for 30 min at room temperature. Radioactivity in this fraction was measured by liquid scintillation.

*Statistical Analysis*—Data were expressed as a mean ± S.E. An unpaired two-tailed Student's *t* test was used for evaluation between the two groups. For comparisons among more groups, statistical significance was assessed using one-way analysis of variance, and the significance of each difference was determined by post hoc testing using the Tukey-Kramer method. Statistical significance was considered at $p < 0.05$.

## RESULTS

*LKB1-KO Mice Exhibit Atrial and Ventricular Hypertrophy*—For this study, we analyzed male LKB1-KO mice and male littermate floxed homozygous mice as control. LKB1 mRNA and protein expression were significantly suppressed by >70% in both the atria and the ventricles of LKB1-KO mice compared with control mice (supplemental Fig. 1). Because the myocyte-specific expression of the α-MHC-Cre strain is well characterized (24), the lack of complete LKB1 ablation may be due to the contribution of LKB1 expressed in non-myocytes (fibroblasts, endothelial cells, and smooth muscle cells) in these hearts. The appearance of excised hearts from 4- and 12-week-old mice is shown in the *top panel* of Fig. 1*A*. By gross inspection, biatrial enlargement was visible at 4 weeks in the LKB1-KO mice compared with control mice. Similarly, by 12 weeks of age, both left and right atria and ventricles were visibly larger in LKB1-KO mice, and there was evidence of thrombus formation in the atria (data not shown). The atria to body weight ratio of LKB1-KO mice was significantly larger compared with control mice at both 4 and 12 weeks (Fig. 1*A*). Although there was no difference of the ventricular weight to body weight ratio at 4 weeks, by 12 weeks the ventricles of the LKB1-KO mice displayed an increase in mass. Similarly, the lung weight to body weight ratio was significantly greater in LKB1-KO mice than in control mice at 12 weeks, but not 4 weeks (data not shown).

Histomorphometric analyses revealed that the diameter of myocytes in the left atria was significantly larger in LKB1-KO mice than in control mice at both 4 weeks and 12 weeks (Fig. 1*B*). Consistent with the chamber weights, there was no difference in left ventricular myocyte diameter at 4 weeks, but this parameter was greater in LKB1-KO mice at 12 weeks of age. Atrial fibrosis was apparent in the atria of LKB1-KO mice at 12 weeks of age (Fig. 1*B*). In addition, collagen type I and III transcripts were elevated in atria of LKB1-KO mice at both 4 and 12 weeks of age compared with controls (Fig. 1*C*). Little or no fibrosis or collagen expression was detected in the ventricles of LKB1-KO mice at 4 or 12 weeks of age.

*LKB1 Deficiency Impairs Cardiac Function*—Echocardiographic analyses were performed to evaluate cardiac structure and function. As shown in Fig. 2, *A* and *B*, left atrial dimension was increased with age in weeks and was markedly enlarged at 12 weeks in LKB1-KO mice compared with control mice. Although there were no differences in left ventricular structure between control mice and LKB1-KO mice at 4 weeks, fractional

shortening, a marker of cardiac systolic function, was significantly reduced in LKB1-KO mice compared with control mice at this time point. By 8 weeks of age, LKB1-KO mice displayed left ventricular diastolic dilatation, and there was evidence of left ventricular hypertrophy in addition to cardiac systolic dysfunction (Fig. 2*B*).

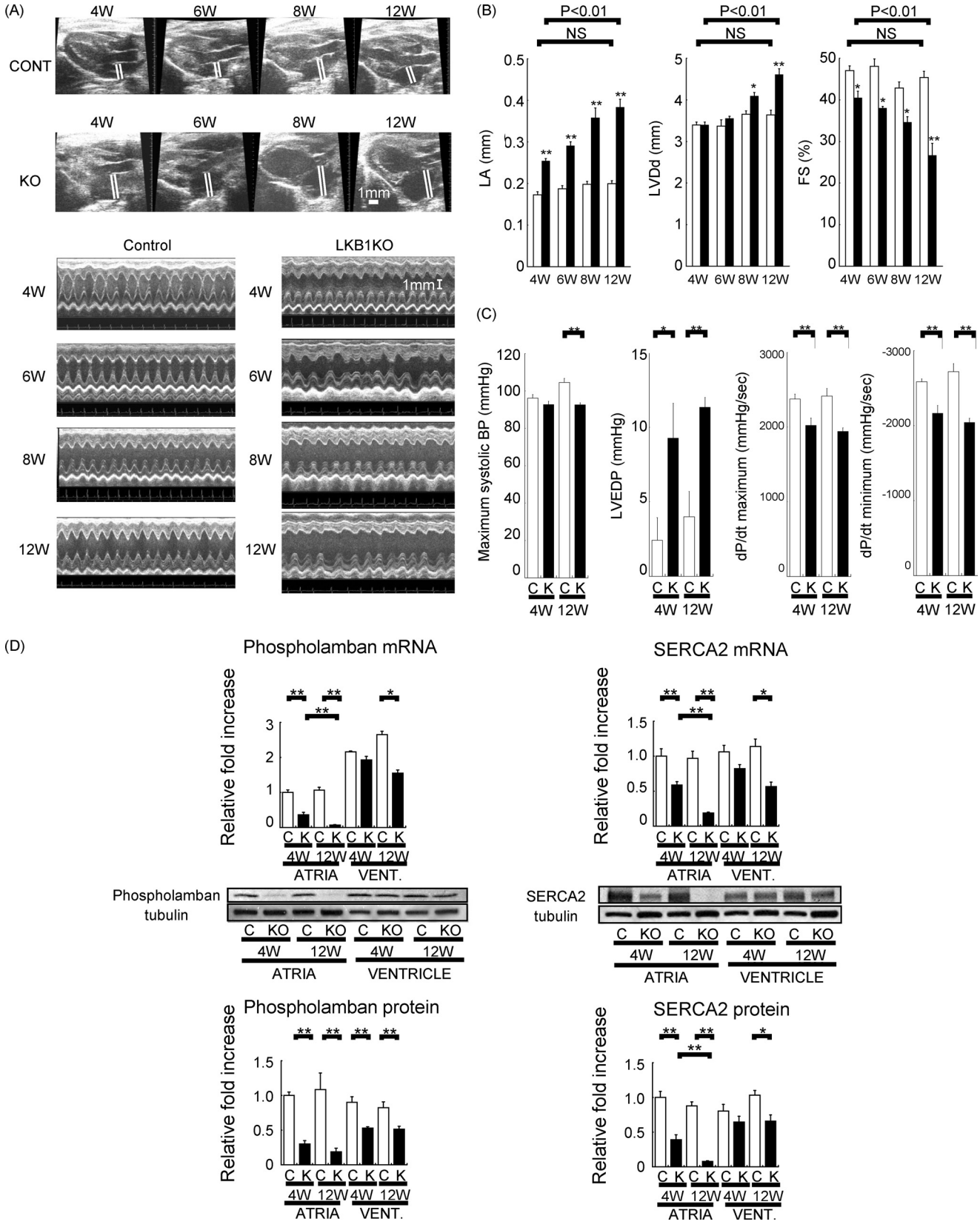

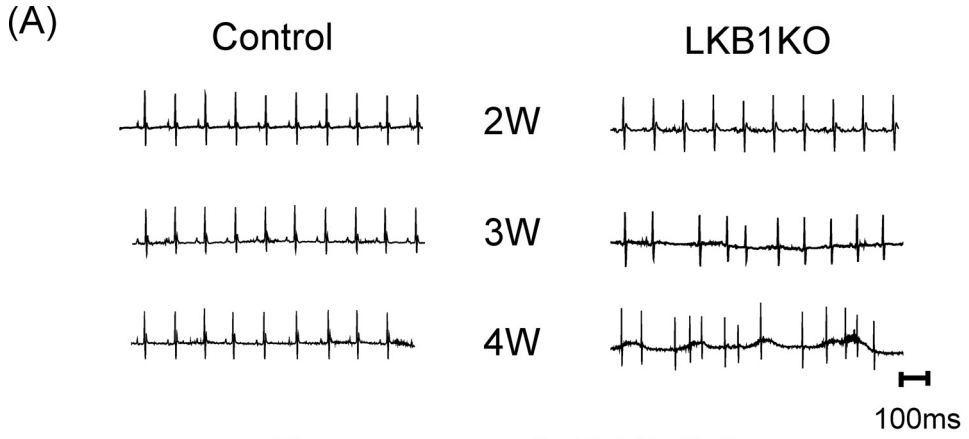


The occurrence of atrial fibrillation

| | Control | LKB1KO |
|---|---|---|
| 4W | 0/20 (0%) | 16/20(80%) |

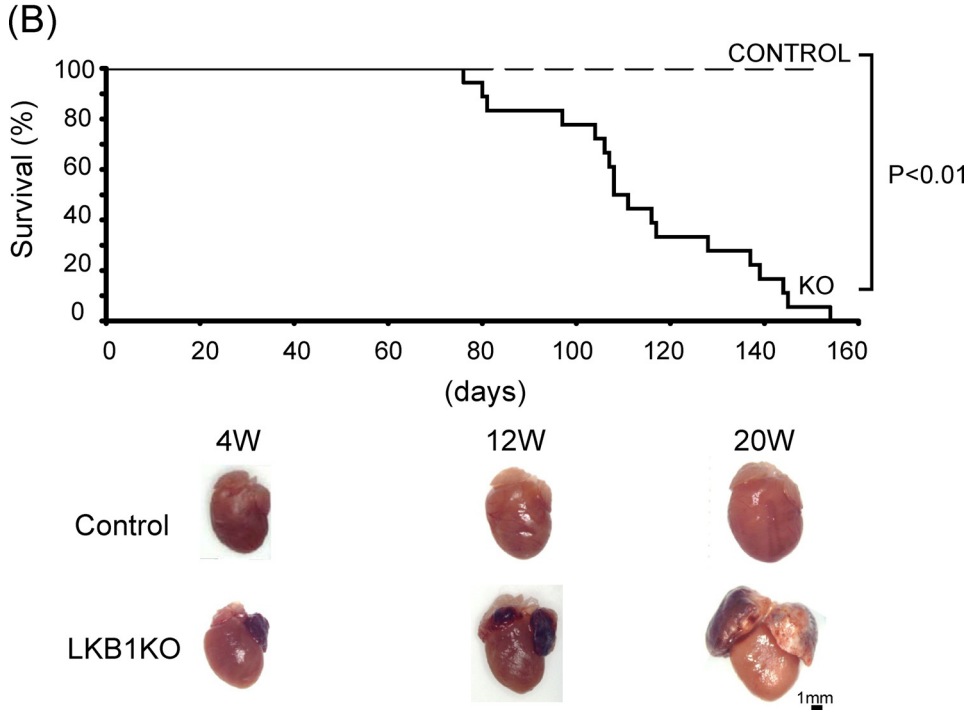


FIGURE 3. **Electrocardiographic assessment and survival of control and LKB1-KO mice.** *A*, representative electrocardiogram showing control mice and LKB1-KO mice at 2, 3, and 4 weeks of age. Control mice presented normal sinus rhythm, whereas LKB1-KO mice presented Afib. Afib occurred in 80% LKB1-KO mice by 4 weeks of age. *B*, mortality rate of control mice and LKB1-KO mice. Mortality curves were created by the Kaplan-Meier method and compared by the log-lank test. $n = 20$ in each group.

Cardiac function was further analyzed by invasive cardiac catheter measurements. Left ventricular end-diastolic pressure was elevated in LKB1-KO mice at 4 weeks of age, left ventricular dP/dt maximum was reduced, and left ventricular dP/dt minimum was increased in LKB1-KO mice (Fig. 2*B*). Systolic blood pressure was significantly decreased in LKB1-KO mice compared with control mice at 12 weeks but not 4 weeks of age. Protein and mRNA expression of SERCA2 and phospholamban were also significantly reduced in both atria and ventricles of LKB1-KO mice compared with control mice (Fig. 2*C*). Together, these findings demonstrate atrial dilatation and left ventricular hypertrophy with cardiac dysfunction in LKB1-KO mice at 4 and 12 weeks of age, respectively.

*Atrial Fibrillation in LKB1-KO Mice*—Because LKB1-KO mice exhibited arrhythmias during echocardiographic and Millar catheter analyses, we assessed whether atrial fibrillation (Afib) occurred in LKB1-KO mice. Electrocardiographic analysis revealed that heart rates in LKB1-KO mice were comparable with that of control mice, and there was no detectable Afib in LKB1-KO mice at 2 or 3 weeks of age. However, ~80% of LKB1-KO mice developed Afib at 4 weeks of age, and all of LKB1-KO mice had Afib at 5 weeks of age or later (Fig. 3*A*). The development of Afib in LKB1-KO mice correlated with the appearance of pronounced atrial hypertrophy. Based upon the gradual onset of the pathologies as well as echocardiographic and histological analysis, Afib in LKB1-KO mice did not appear to result from congenital cardiac abnormalities such as atrial or ventricular septal defects.

*Mortality of LKB1-KO Mice*—Consistent with poor cardiac performance in LKB1-KO mice, the mortality of male LKB1-KO mice was notable after 12 weeks of age. All LKB1-KO mice had died by 5 months of age, and the mean survival period was 110 days (Fig. 3*B*). Although female

FIGURE 2. **Direct and indirect measures of cardiac dysfunction in LKB1-KO mice at 4 and 12 weeks of age.** *A*, representative echocardiogram. Serial changes of B-mode of parasternal long axis view and M-mode of left ventricular short axis view in control and LKB1-KO mice are shown. *B*, echocardiographic measurements of left atrial dimension (*LA*), left ventricular diastolic dimension (*LVDd*), and fractional shortening (*FS*) between 4- and 12-week-old control and LKB1-KO mice. *, $p < 0.05$; **, $p < 0.01$ *versus* age-matched control; $n = 8$ in each sample. *NS*, not significant. *C*, invasive analysis of cardiac function with Miller catheter in both 4- and 12-week-old control and LKB1-KO mice. Values are expressed as mean ± S.E. *, $p < 0.05$; **, $p < 0.01$. Each group $n = 8$. *BP*, blood pressure. *D*, mRNA and protein expression of phospholamban and SERCA2. The real time PCR or Western blot analyses were performed in control (*open bars*) and LKB1-KO (*filled bars*) at 4 and 12 weeks of age, respectively. Values are change relative to each control band (4-week-old control atria) and are expressed as mean ± S.E. *, $p < 0.05$; **, $p < 0.01$; $n = 6–8$ in each group.

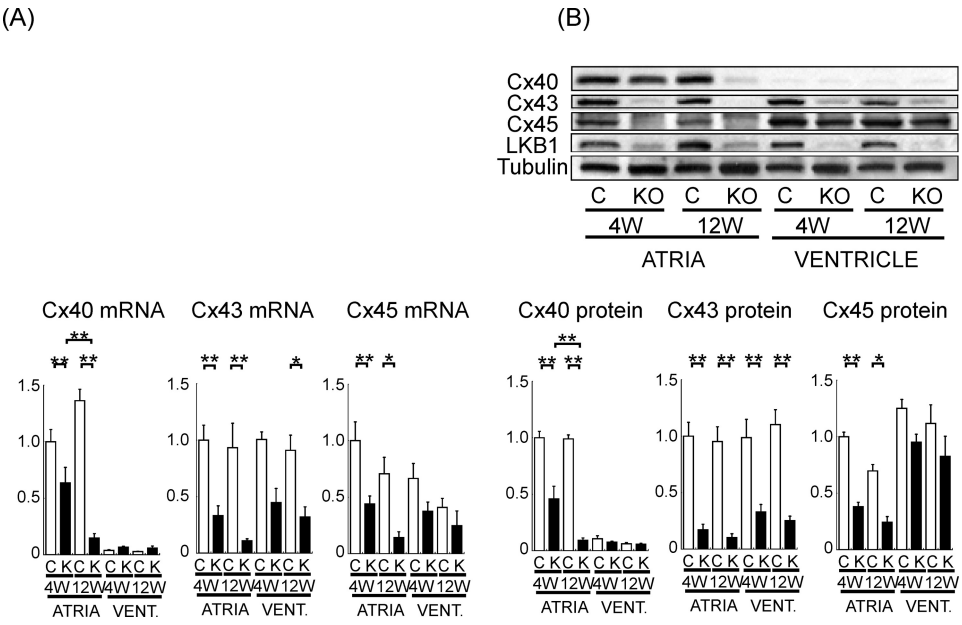


FIGURE 4. **mRNA and protein expression of connexin 40, 43, and 45.** *A*, results of real time PCR analysis of connexin 40, 43, and 45. Values are change relative to each control (using atria at 4 weeks of age as control) and expressed as mean ± S.E. *, $p < 0.05$; **, $p < 0.01$, $n = 6$ in each group. *B*, *upper*, representative immunoblots of connexin 40, 43, and 45 in atria and ventricles of control mice and LKB1-KO mice. *Lower*, densitometric analysis of connexin 40, 43, and 45. The expression levels were quantified and are expressed as change relative to 4-week-old control atria. Values are change relative to each control (using atria at 4 weeks of age as control) and are expressed as mean ± S.E. *, $p < 0.05$; **, $p < 0.01$, $n = 6$ in each group.

LKB1-KO lived longer than male LKB1-KO mice, all died by 1 year of age (data not shown).

*Reduced Expression of Gap Junction Proteins in Atria and Ventricle of LKB1-KO Mice*—Because gap junction proteins have been reported to participate in the occurrence of Afib (25), we examined the expression of connexin 40, 43, and 45 in atria and ventricles in control and LKB1-KO mice. The expression of connexin 40, 43, and 45 mRNA and protein was significantly decreased in atria of LKB1-KO at both 4 and 12 weeks compared with that of control mice (Fig. 4). Connexin 43 was also significantly reduced in the ventricles of LKB1-KO mice (Fig. 4).

*Capillary Density Is Reduced in Atria and Ventricle of LKB1-KO Mice*—Cardiac microvasculature mediated by the VEGF pathway plays an important role in the maintenance of cardiac function (26) or the transition from compensatory hypertrophy to heart failure (27, 28). Therefore, we evaluated capillary density in heart by performing immunohistochemistry for CD31 in cardiac tissue sections. Capillary density was significantly decreased in both atria and ventricles of LKB1-KO mice compared with control mice (Fig. 5*A*). This reduction in capillary density was more pronounced at 12 weeks than at 4 weeks of age. As shown in Fig. 5*B*, mRNA and protein levels of VEGF expression were also reduced in both atria and ventricles of LKB1-KO mice.

*Reduced AMPK and eEF2 Phosphorylation and Increased mTOR/p70S6 Kinase Signaling in LKB1-KO Mouse Heart*—To determine the effects of LKB1 ablation on AMPK signaling, the phosphorylation of AMPK and ACC, a downstream target of AMPK, was examined by Western immunoblot analysis in hearts from LKB1-KO and control mice (Fig. 6*A*). Phosphorylation of AMPK at $Thr^{172}$ and ACC at $Ser^{79}$ was significantly suppressed in both atria and ventricles of LKB1-KO mice at both 4 and 12 weeks of age. In contrast, the phosphorylation of Akt at $Ser^{473}$, a mediator of cardiac hypertrophy (28), was not affected. Because the phenotype of the LKB1-KO mice is similar to the phenotype of cardiac-specific dominant negative CREB transgenic mice (29, 30), we also examined the phosphorylation status of CREB. CREB phosphorylation at $Ser^{133}$ was significantly reduced in atria and ventricles of LKB1-KO mice compared with control mice at both 4 and 12 weeks of age (Fig. 6*A*). Other master regulators of protein synthesis such as mTOR and p70S6 kinase also demonstrated augmented activating phosphorylation in LKB1-KO mice compared with control mice (Fig. 6*B*). The phosphorylation of eEF2 at $Thr^{56}$ was decreased in LKB1-KO mice. Because reduced phosphorylation at this residue allows eEF2 to catalyze the translocation step involved in protein synthesis (31), this finding is indicative of increased protein synthesis necessary for cardiac hypertrophy (32).

*LKB1 Regulation of Myocyte Hypertrophy in Vitro*—To confirm that loss of LKB1 activity was responsible for the development of cardiac hypertrophy, we utilized an siRNA ablation procedure in cultured neonatal rat cardiac myocytes. Transfection of siRNA targeting LKB1 led to an 80% reduction in LKB1 expression (data not shown), which correlated with cardiac myocyte hypertrophy assessed by cell surface area and [$^3$H]-leucine incorporation (Fig. 7, *A–C*). Consistent with the development of cardiac hypertrophy induced by decreased LKB1, LKB1 ablation by siRNA also led to elevations of A-type natriuretic peptide, B-type natriuretic peptide, and $\alpha$-smooth muscle actin mRNA expression (Fig. 7*D*). Importantly, transduction with Ad-caAMPK or treatment with the mTOR inhibitor rapamycin reversed the hypertrophic effects of siRNA targeting LKB1 (Fig. 7, *E–G*). In contrast, transduction with Ad-DCREB had no effect on hypertrophy induced by siRNA targeting LKB1 (Fig. 7, *H–J*). Although CREB is reported to be a downstream target of AMPK (33), we found that transduction with Ad-caAMPK did not influence CREB phosphorylation, and transduction with Ad-DCREB did not influence AMPK phosphorylation (data not shown).

## DISCUSSION

Although LKB1 was originally identified as a tumor suppressor (6) and has been associated with proteins that are involved in controlling cellular proliferation (34–37), LKB1 has also been shown to phosphorylate and activate AMPK (38), a negative regulator of cardiac growth. As a result, many of the cellular effects attributed to AMPK may be indirectly mediated by LKB1. Because AMPK plays a role in the regulation of cardiac

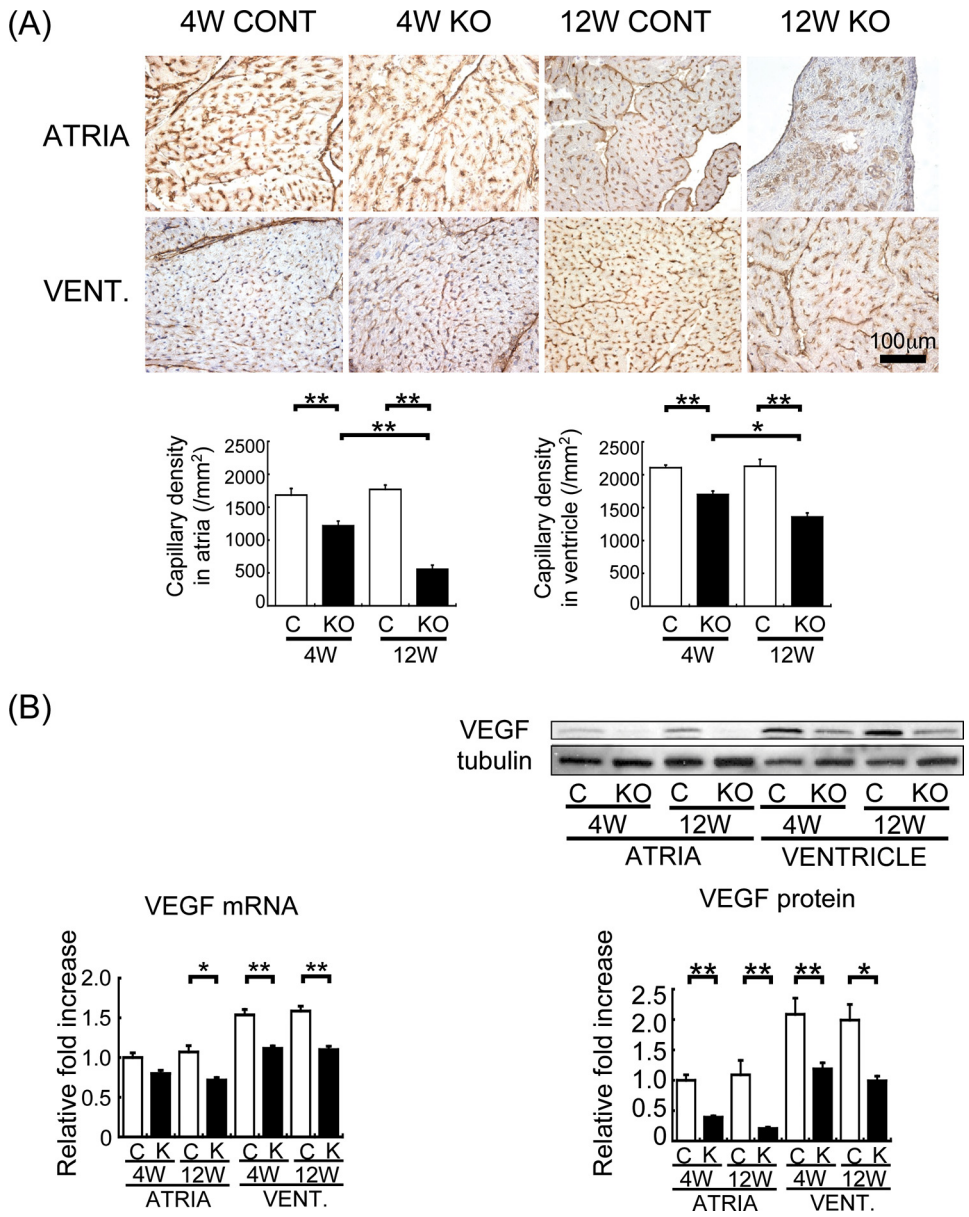


FIGURE 5. **Capillary density in both atria and ventricles from control and LKB1-KO mice at 4 and 12 weeks of age.** *A*, *top* and *middle panels*, representative histological sections of CD31 immunohistochemistry staining in atria and ventricles. *Bottom panel*, mean capillary density in control (*open bars*) and LKB1-KO (*filled bars*) mice. Values are expressed as mean ± S.E. *, $p < 0.05$; **, $p < 0.01$; $n = 4–6$ in each group. *B*, mRNA (*left*) levels and protein levels with the representative blots (*right*) of VEGF expression in atria and ventricles. Values are expressed as mean ± S.E. *, $p < 0.05$; **, $p < 0.01$, $n = 6–8$ in each group.

function and metabolism as well as cardiac myocyte cell growth (39, 40), the importance of LKB1/AMPK signaling in cardiac physiology and pathophysiology is receiving increasing attention. Here, we present an in-depth investigation of the role of LKB1 signaling in the mouse heart using cardiac myocyte-specific LKB1-KO mice.

Using a newly created mouse strain that lacks LKB1 expression in cardiac myocytes, we performed gross morphometric and histological analysis of the myocardium at 4 and 12 weeks of age. Consistent with a previous report using the conditional KO for muscle LKB1 (12), we observed biatrial enlargement in our LKB1-KO. However, in contrast to that previous report (12), cardiac myocyte-specific LKB1-KO mice displayed an increase in both atrial and ventricular myocyte diameter. In accordance with a more severe and progressive pathological cardiac phenotype observed in the cardiac myocyte-specific LKB1-KO mice, there was significant reduction in cardiac systolic function in the LKB1-KO mice compared with controls, a finding that was absent in the MCK-Cre strain (12). The cardiac myocyte-specific LKB1-KO also displayed Afib, a phenotype that was not reported in the muscle LKB1-KO (12). There are a number of possible reasons that can explain why the cardiac phenotype of the conditional KO for muscle LKB1 is different from the phenotype reported here. For instance, the ablation of muscle LKB1 may indirectly influence cardiac development via an unidentified skeletal muscle-specific mechanism. Alternatively, the timing of expression of the Cre during development may alter the timing of LKB1 ablation, thus altering the cardiac phenotype. In addition, the conditional muscle LKB1-KO mice were generated from a different strain of floxed mice (4, 12), and this may also contribute to the differences between these two mouse models. Regardless of the reasons for the different phenotypes, the cardiac myocyte-specific LKB1-KO mice used in the present study demonstrated a severe cardiac phenotype characterized by biatrial enlargement, left ventricular hypertrophy, and increased fibrosis and collagen content as well as cardiac dysfunction. Together, these findings suggest that LKB1 plays a more important role in maintaining cardiac structure and function than was previously appreciated.

Based on the severe adverse cardiac phenotype observed in LKB1-KO mice by morphometric and histological analysis, we further characterized the cellular components that may be involved in the progressive atrial dilatation. Consistent with atrial dysfunction and the potential for altered calcium handling, SERCA2 and phospholamban protein levels were significantly reduced in atria of LKB1-KO mice. Because abnormal calcium handling influences atrial contractility and can promote arrhythmogenesis (41), we also performed electrocardiographic analysis of hearts from LKB1-KO mice. In agreement with atrial enlargement preceding cardiac arrhythmia (30, 42–45), LKB1-KO mice developed Afib at 4 weeks of age when atrial hypertrophy was already evident. In

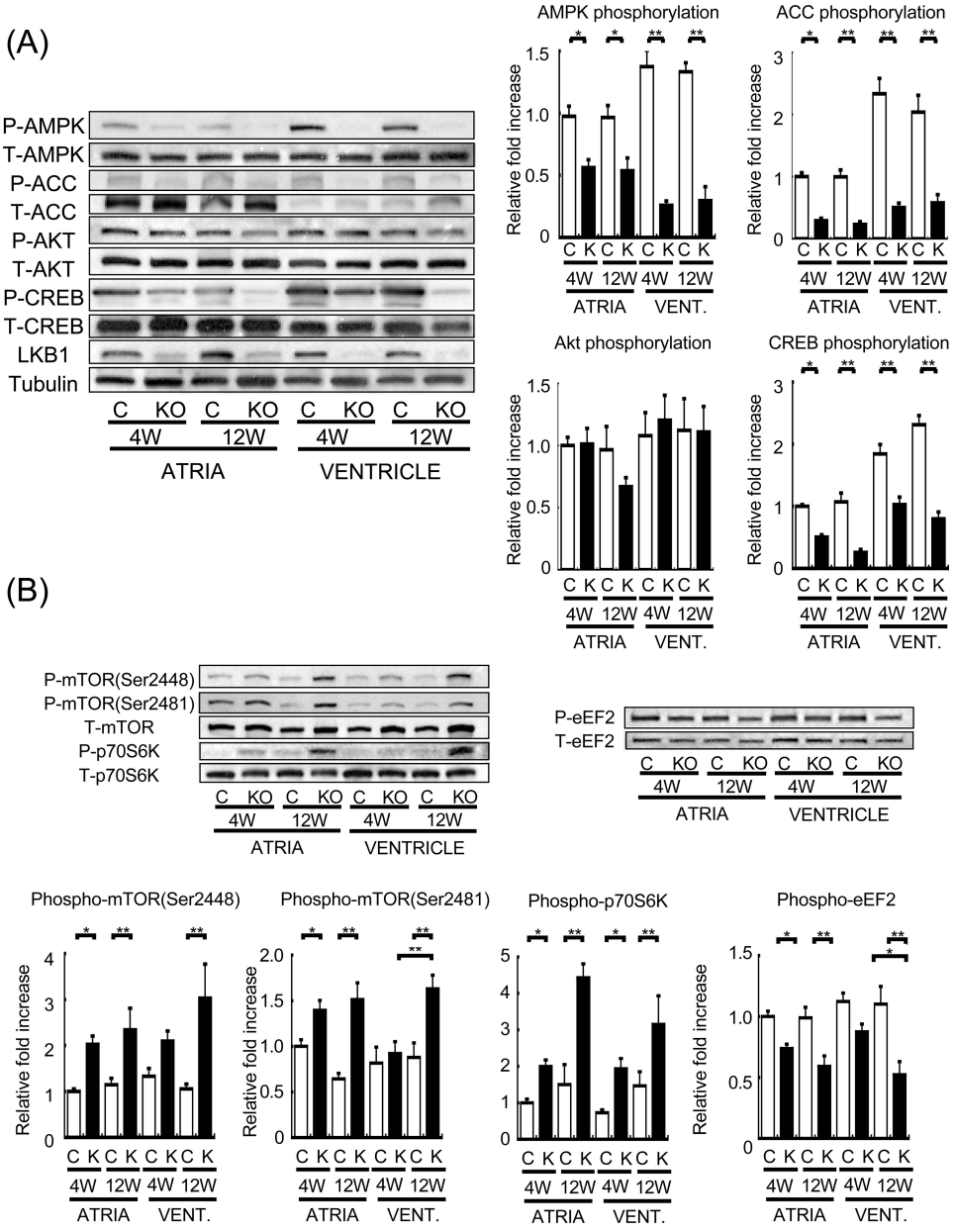


FIGURE 6. **Phosphorylation level of AMPK, ACC, CREB, and Akt in both atria and ventricles from control and LKB1-KO mice.** *A*, *left*, representative blot of phosphorylated and total AMPK (*pAMPK* and *tAMPK*, respectively), phosphorylated and total ACC (*pACC* and *tACC*, respectively), phosphorylated and total Akt (*pAKT* and *tAKT*, respectively), and phosphorylated and total CREB (*pCREB* and *tCREB*, respectively). *Right*, results of densitometric analysis of ACC, AMPK, Akt, and CREB phosphorylation. *B*, phosphorylation level of mTOR, p70S6 kinase, and eEF2 in atria and ventricles from control and LKB1-KO mice. *Upper*, representative blot of phospho- and total mTOR, p70S6 kinase and eEF2. *Lower*, densitometric analysis of mTOR, p70S6 kinase, and eEF2 phosphorylation. The phosphorylation levels were quantified and are expressed as change relative to each control band (atria from control mice at 4 weeks of age). Values shown are mean ± S.E. *, $p < 0.05$; **, $p < 0.01$; $n = 8$ in each group.

addition, we found that gap junction proteins such as Cx40, Cx43, and Cx45 were significantly decreased in both atria and ventricles of LKB1-KO mice, and these decreases may also predispose the heart to abnormal conduction and arrhythmia (46). Based on these findings, we propose that fatal arrhythmias may contribute to the high mortality rate of the LKB1-KO mice. Taken together, atrial enlargement, altered expression of calcium handling proteins, and the degradation of connexin expression likely contribute to the occurrence of Afib in LKB1-KO mice. However, whether or not these are the only contributors to Afib in the LKB1-KO mice has yet to be established.

AMPK is a negative regulator of protein synthesis in cardiac myocytes (32). Consistent with this notion, the enlarged LKB1-deficient hearts displayed reductions in AMPK signaling. However, in addition to AMPK, LKB1 also targets members of an AMPK-related superfamily including BRSK1, BRSK2, NUAK1, NUAK2, QIK, QSK, SIK, MARK1, MARK2, MARK3, MARK4, and SNRK (1). Furthermore, AMPK is regulated by multiple upstream protein kinases, including $Ca^{2+}$/calmodulin-dependent protein kinase kinase-$\beta$ (CaMKK$\beta$) and transforming growth factor-$\beta$-activated kinase 1 (TAK1) in addition to LKB1 (47). Because both LKB1 and AMPK participate in complex regulatory networks, one cannot assume *a priori* that the hypertrophy observed in the cardiac-specific LIKB1-KO mice is due to a reduction in AMPK activity. Therefore, we investigated whether LKB1 ablation resulted in impaired AMPK activation and a subsequent activation of prohypertrophic signaling pathways in cultured myocytes. Loss of LKB1 resulted in reduced AMPK activity and a corresponding activation of signaling pathways that are major regulators of protein synthesis, namely mTOR, p70S6 kinase, and eEF2 (48). Inhibition of LKB1/AMPK signaling and a subsequent activation of the mTOR/p70S6 kinase signaling axis have been proposed to create a permissive environment that promotes hypertrophic growth (15). Consistent with this notion, the mTOR/P70S6 kinase/eEF2 signaling cascade is activated in hearts from LKB1-KO mice, which may contribute to atrial and ventricular hypertrophy in these mice. We also showed that cardiac hypertrophy induced by siRNA ablation of LKB1 in cultured cardiac myocytes was prevented by genetic activation of AMPK as well as pharmacological inhibition of the mTOR pathway. Collectively, these data suggest that the cardiac hypertrophy induced by the loss of LKB1 activity is in part mediated by a downstream hierarchical kinase cascade involving AMPK and mTOR.

In contrast to LKB1-deficient mice, no baseline cardiac hypertrophy has been reported for mice that are deficient for

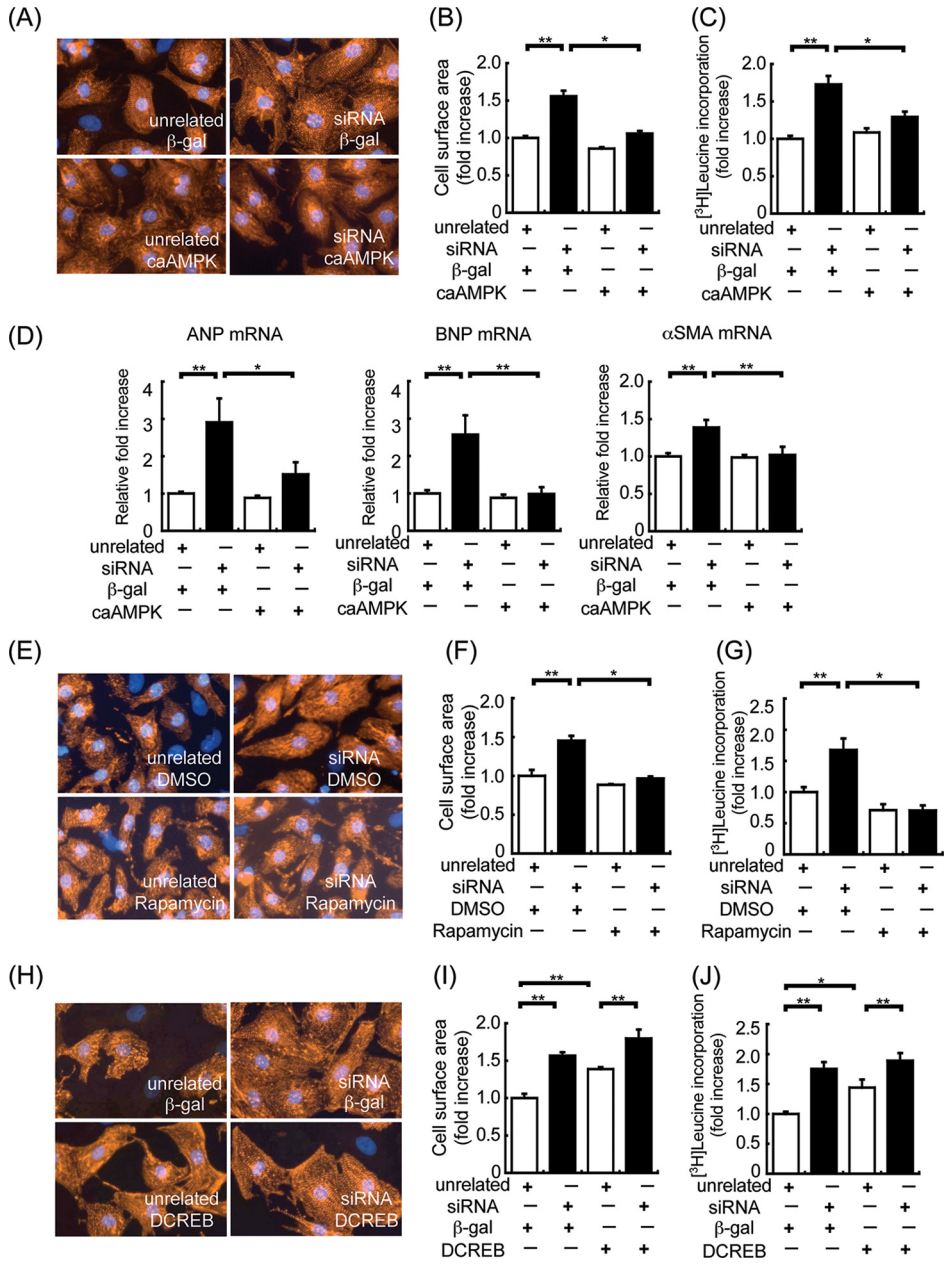


FIGURE 7. **Assessment of LKB1 siRNA-induced cardiac myocyte hypertrophy.** LKB1 siRNA-induced cardiac myocyte hypertrophy was inhibited by caAMPK, not DCREB, *in vitro*. *A*, representative cell size of cardiac myocytes transfected with unrelated siRNA (control) or LKB1 siRNA for 48 h. After 24 h of siRNA transfection, cardiac myocytes were transfected with β-galactosidase (*β-gal*) or caAMPK adenovirus. Cardiac myocytes were stained with α-actinin for quantification of cell surface area. *B*, quantitative analysis of cell surface area after siRNA transfection with or without caAMPK adenovirus infection. *, $p < 0.05$; **, $p < 0.01$; $n = 4$ in each group. *C*, [$^3$H]leucine incorporation for assessment of protein synthesis in cardiac myocytes. The measurement of radioactivity in cardiac myocytes after siRNA transfection with or without caAMPK adenovirus infection is shown. *, $p < 0.05$; **, $p < 0.01$; $n = 8$–12 in each group. *D*, results of real time PCR analysis of A-type natriuretic peptide (*ANP*), B-type natriuretic peptide (*BNP*), and α-smooth muscle actin (*α-SMA*), expression with control or siRNA in the presence of β-galactosidase or caAMPK adenovirus. *, $p < 0.05$; **, $p < 0.01$; $n = 6$ in each group. *E*, representative cell size of cardiac myocytes transfected with unrelated siRNA (control) or LKB1 siRNA for 48 h. After 24 h of siRNA transfection, cardiac myocytes were treated with vehicle (*DMSO*) or rapamycin. Cardiac myocytes were stained with α-actinin for quantification of cell surface area. $n = 4$ in each group. *F*, quantitative analysis of cell surface area after siRNA transfection with or without rapamycin treatment. *, $p < 0.05$; **, $p < 0.01$; $n = 4$ in each group. *G*, [$^3$H]leucine incorporation for assessment of protein synthesis in cardiac myocytes. The measurement of radioactivity in cardiac myocytes after siRNA transfection with or without rapamycin treatment is shown. *, $p < 0.05$; **, $p < 0.01$; $n = 6$–8 in each group. *H*, representative cell size of cardiac myocytes transfected with unrelated siRNA (control) or LKB1 siRNA for 48 h. Cardiac myocytes were stained with α-actinin for quantification of cell surface area. $n = 4$ in each group. *I*, quantitative analysis of cell surface area after siRNA transfection with or without DCREB adenovirus infection. **, $p < 0.01$; $n = 4$ in each group. *J*, [$^3$H]leucine incorporation for assessment of protein synthesis in cardiac myocytes. The measurement of radioactivity in cardiac myocytes after siRNA transfection with or without DCREB adenovirus infection is shown. *, $p < 0.05$; **, $p < 0.01$; $n = 8$–12 in each group. In all *panels*, values are expressed as mean ± S.E.

AMPKα1 (49) or AMPKα2 (50) or that express a dominant negative form of AMPKα2 expressed from MCK or α-MHC promoters (51, 52). However, AMPKα2-KO mice are reported to exhibit a modest increase in left ventricular hypertrophy compared with wild-type in response to pressure overload (53). At least two explanations can account for the discrepancy between the subtle phenotype seen with the AMPK stains and the pronounced cardiac phenotype in the LKB1-KO mouse line that is reported here. First, it is possible that functional compensation between the AMPKα1 and α2 subunits minimizes the cardiac phenotype, whereas a lack of LKB1 leads to the simultaneous dysregulation of both isoforms. However, it is equally plausible that other, as yet unidentified, downstream targets of LKB1 participate in the cardiac remodeling process in an AMPK-independent manner. Thus, additional studies will be required to address the relative contributions of AMPKα1/α2 *versus* other AMPK family kinases that function downstream of LKB1 in heart.

The phenotype of atrial dilatation and a conduction system abnormality in the cardiac myocyte-specific LKB1-KO mouse model was similar to that of mice expressing cardiac-specific dominant negative CREB (29, 30). Thus, we investigated whether CREB phosphorylation was inhibited in hearts of LKB1-KO mice. CREB phosphorylation was diminished in both atria and ventricles of LKB1-KO mice as well as in cultured cardiac myocytes treated with siRNA directed to LKB1. Although these data suggest that reduced CREB activity is involved in the atrial phenotype of the LKB1-KO mice, expression of constitutively active CREB failed to attenuate LKB1 siRNA-induced cardiac myocytes hypertrophy in our cell culture system. Although these data suggest that the cardiac phenotype observed in our model is independent from an LKB1-mediated effect on CREB, further studies on

a possible connection between LKB1 and CREB in cardiac myocytes is warranted.

In contrast to muscle LKB1-KO mice, cardiac myocyte-specific LKB1-KO mice exhibited cardiac dysfunction. In the heart, VEGF-mediated microvasculature is required to maintain cardiac function (26), and the reduction in capillary density mediated by a disruption in VEGF signaling contributes to the transition from compensatory hypertrophy to heart failure (27, 28). Because VEGF signaling plays a crucial role in regulating cardiac function during growth, we examined VEGF expression and capillary density in cardiac-specific LKB1-KO mice. We demonstrated that VEGF protein and mRNA expression were reduced in both atria and ventricles of LKB1-KO mice. Consistent with these observations, capillary densities were markedly reduced in both atria and ventricles of LKB1-KO mice, and these effects were observed as early as 4 weeks of age. Previously, we have shown that AMPK activation promotes VEGF expression and angiogenesis in skeletal muscle (54). Taken together, these data suggest that LKB1 promotes angiogenesis and maintains function in the developing heart through activation of the AMPK/VEGF signaling axis within cardiac myocytes.

In summary, we show that the loss of LKB1 in cardiac myocytes induces aberrant remodeling of both the atria and ventricles with cardiac dysfunction at base line. The cardiac remodeling observed in the LKB1-deficient hearts was also associated with a reduction in capillary density and VEGF expression in the atria and ventricles. Moreover, LKB1 ablation promoted the development of Afib and reductions in gap junction protein expression. We also show that the hypertrophy of the atria and ventricles was associated with diminished AMPK activation and the dysregulation of the mTOR/p70S6 kinase/eEF2 signaling axis. In cultured myocytes, the loss of LKB1 could be rescued by either restoration of AMPK activity or inhibition of mTOR/p70S6 kinase signaling. Together, these findings highlight the importance of LKB1 signaling in the heart and provide further evidence supporting the notion that the loss of LKB1 is prohypertrophic and may be involved in the development of pathological cardiac hypertrophy.

## REFERENCES


1. Lizcano, J. M., Göransson, O., Toth, R., Deak, M., Morrice, N. A., Boudeau, J., Hawley, S. A., Udd, L., Mäkelä, T. P., Hardie, D. G., and Alessi, D. R. (2004) *EMBO J.* **23,** 833–843
2. Ylikorkala, A., Rossi, D. J., Korsisaari, N., Luukko, K., Alitalo, K., Henkemeyer, M., and Mäkelä, T. P. (2001) *Science* **293,** 1323–1326
3. Shaw, R. J., Lamia, K. A., Vasquez, D., Koo, S. H., Bardeesy, N., Depinho, R. A., Montminy, M., and Cantley, L. C. (2005) *Science* **310,** 1642–1646
4. Sakamoto, K., McCarthy, A., Smith, D., Green, K. A., Grahame Hardie, D., Ashworth, A., and Alessi, D. R. (2005) *EMBO J.* **24,** 1810–1820
5. Koh, H. J., Arnolds, D. E., Fujii, N., Tran, T. T., Rogers, M. J., Jessen, N., Li, Y., Liew, C. W., Ho, R. C., Hirshman, M. F., Kulkarni, R. N., Kahn, C. R., and Goodyear, L. J. (2006) *Mol. Cell. Biol.* **26,** 8217–8227
6. Hemminki, A., Markie, D., Tomlinson, I., Avizienyte, E., Roth, S., Loukola, A., Bignell, G., Warren, W., Aminoff, M., Höglund, P., Järvinen, H., Kristo, P., Pelin, K., Ridanpää, M., Salovaara, R., Toro, T., Bodmer, W., Olschwang, S., Olsen, A. S., Stratton, M. R., de la Chapelle, A., and Aaltonen, L. A. (1998) *Nature* **391,** 184–187
7. Jenne, D. E., Reimann, H., Nezu, J., Friedel, W., Loff, S., Jeschke, R., Müller, O., Back, W., and Zimmer, M. (1998) *Nat. Genet.* **18,** 38–43
8. Marignani, P. A. (2005) *J. Clin. Pathol.* **58,** 15–19
9. Noga, A. A., Soltys, C. L., Barr, A. J., Kovacic, S., Lopaschuk, G. D., and Dyck, J. R. (2007) *Am. J. Physiol. Heart Circ. Physiol.* **292,** H1460–H1469
10. Xie, M., Zhang, D., Dyck, J. R., Li, Y., Zhang, H., Morishima, M., Mann, D. L., Taffet, G. E., Baldini, A., Khoury, D. S., and Schneider, M. D. (2006) *Proc. Natl. Acad. Sci. U.S.A.* **103,** 17378–17383
11. Chan, A. Y., Dolinsky, V. W., Soltys, C. L., Viollet, B., Baksh, S., Light, P. E., and Dyck, J. R. (2008) *J. Biol. Chem.* **283,** 24194–24201
12. Sakamoto, K., Zarrinpashneh, E., Budas, G. R., Pouleur, A. C., Dutta, A., Prescott, A. R., Vanoverschelde, J. L., Ashworth, A., Jovanoviæ, A., Alessi, D. R., and Bertrand, L. (2006) *Am. J. Physiol. Endocrinol. Metab.* **290,** E780–E788
13. Johnson, J. E., Wold, B. J., and Hauschka, S. D. (1989) *Mol. Cell. Biol.* **9,** 3393–3399
14. Shield, M. A., Haugen, H. S., Clegg, C. H., and Hauschka, S. D. (1996) *Mol. Cell. Biol.* **16,** 5058–5068
15. Dolinsky, V. W., Chan, A. Y., Robillard Frayne, I., Light, P. E., Des Rosiers, C., and Dyck, J. R. (2009) *Circulation* **119,** 1643–1652
16. Bardeesy, N., Sinha, M., Hezel, A. F., Signoretti, S., Hathaway, N. A., Sharpless, N. E., Loda, M., Carrasco, D. R., and DePinho, R. A. (2002) *Nature* **419,** 162–167
17. Ikeda, Y., Aihara, K., Sato, T., Akaike, M., Yoshizumi, M., Suzaki, Y., Izawa, Y., Fujimura, M., Hashizume, S., Kato, M., Yagi, S., Tamaki, T., Kawano, H., Matsumoto, T., Azuma, H., Kato, S., and Matsumoto, T. (2005) *J. Biol. Chem.* **280,** 29661–29666
18. Shibata, R., Sato, K., Pimentel, D. R., Takemura, Y., Kihara, S., Ohashi, K., Funahashi, T., Ouchi, N., and Walsh, K. (2005) *Nat. Med.* **11,** 1096–1103
19. Ikeda, Y., Ohashi, K., Shibata, R., Pimentel, D. R., Kihara, S., Ouchi, N., and Walsh, K. (2008) *FEBS Lett.* **582,** 1147–1150
20. Ohashi, K., Kihara, S., Ouchi, N., Kumada, M., Fujita, K., Hiuge, A., Hibuse, T., Ryo, M., Nishizawa, H., Maeda, N., Maeda, K., Shibata, R., Walsh, K., Funahashi, T., and Shimomura, I. (2006) *Hypertension* **47,** 1108–1116
21. Pimentel, D. R., Adachi, T., Ido, Y., Heibeck, T., Jiang, B., Lee, Y., Melendez, J. A., Cohen, R. A., and Colucci, W. S. (2006) *J. Mol. Cell. Cardiol.* **41,** 613–622
22. Zang, M., Zuccollo, A., Hou, X., Nagata, D., Walsh, K., Herscovitz, H., Brecher, P., Ruderman, N. B., and Cohen, R. A. (2004) *J. Biol. Chem.* **279,** 47898–47905
23. Shiojima, I., Yefremashvili, M., Luo, Z., Kureishi, Y., Takahashi, A., Tao, J., Rosenzweig, A., Kahn, C. R., Abel, E. D., and Walsh, K. (2002) *J. Biol. Chem.* **277,** 37670–37677
24. Gulick, J., and Robbins, J. (2009) *Methods Mol. Biol.* **561,** 91–104
25. Brundel, B. J., Henning, R. H., Kampinga, H. H., Van Gelder, I. C., and Crijns, H. J. (2002) *Cardiovasc. Res.* **54,** 315–324
26. Giordano, F. J., Gerber, H. P., Williams, S. P., VanBruggen, N., Bunting, S., Ruiz-Lozano, P., Gu, Y., Nath, A. K., Huang, Y., Hickey, R., Dalton, N., Peterson, K. L., Ross, J., Jr., Chien, K. R., and Ferrara, N. (2001) *Proc. Natl. Acad. Sci. U.S.A.* **98,** 5780–5785
27. Izumiya, Y., Shiojima, I., Sato, K., Sawyer, D. B., Colucci, W. S., and Walsh, K. (2006) *Hypertension* **47,** 887–893
28. Shiojima, I., Sato, K., Izumiya, Y., Schiekofer, S., Ito, M., Liao, R., Colucci, W. S., and Walsh, K. (2005) *J. Clin. Invest.* **115,** 2108–2118
29. Fentzke, R. C., Korcarz, C. E., Lang, R. M., Lin, H., and Leiden, J. M. (1998) *J. Clin. Invest.* **101,** 2415–2426
30. Zhu, W., and Saba, S. (2003) *J. Cardiovasc. Electrophysiol.* **14,** 982–989
31. Carlberg, U., Nilsson, A., and Nygård, O. (1990) *Eur. J. Biochem.* **191,** 639–645
32. Chan, A. Y., Soltys, C. L., Young, M. E., Proud, C. G., and Dyck, J. R. (2004) *J. Biol. Chem.* **279,** 32771–32779
33. Thomson, D. M., Herway, S. T., Fillmore, N., Kim, H., Brown, J. D., Barrow, J. R., and Winder, W. W. (2008) *J. Appl. Physiol.* **104,** 429–438
34. Karuman, P., Gozani, O., Odze, R. D., Zhou, X. C., Zhu, H., Shaw, R., Brien, T. P., Bozzuto, C. D., Ooi, D., Cantley, L. C., and Yuan, J. (2001) *Mol. Cell* **7,** 1307–1319
35. Marignani, P. A., Kanai, F., and Carpenter, C. L. (2001) *J. Biol. Chem.* **276,** 32415–32418
36. Shaw, R. J., Bardeesy, N., Manning, B. D., Lopez, L., Kosmatka, M., DePinho, R. A., and Cantley, L. C. (2004) *Cancer Cell* **6,** 91–99
37. Smith, D. P., Rayter, S. I., Niederlander, C., Spicer, J., Jones, C. M., and

Ashworth, A. (2001) *Hum. Mol. Genet.* **10,** 2869–2877
38. Hawley, S. A., Boudeau, J., Reid, J. L., Mustard, K. J., Udd, L., Mäkelä, T. P., Alessi, D. R., and Hardie, D. G. (2003) *J. Biol.* **2,** 28
39. Dolinsky, V. W., and Dyck, J. R. (2006) *Am. J. Physiol. Heart Circ. Physiol.* **291,** H2557–H2569
40. Dyck, J. R., and Lopaschuk, G. D. (2006) *J. Physiol.* **574,** 95–112
41. El-Armouche, A., Boknik, P., Eschenhagen, T., Carrier, L., Knaut, M., Ravens, U., and Dobrev, D. (2006) *Circulation* **114,** 670–680
42. Müller, F. U., Lewin, G., Baba, H. A., Boknik, P., Fabritz, L., Kirchhefer, U., Kirchhof, P., Loser, K., Matus, M., Neumann, J., Riemann, B., and Schmitz, W. (2005) *J. Biol. Chem.* **280,** 6906–6914
43. Okamoto, Y., Chaves, A., Chen, J., Kelley, R., Jones, K., Weed, H. G., Gardner, K. L., Gangi, L., Yamaguchi, M., Klomkleaw, W., Nakayama, T., Hamlin, R. L., Carnes, C., Altschuld, R., Bauer, J., and Hai, T. (2001) *Am. J. Pathol.* **159,** 639–650
44. Saba, S., Janczewski, A. M., Baker, L. C., Shusterman, V., Gursoy, E. C., Feldman, A. M., Salama, G., McTiernan, C. F., and London, B. (2005) *Am. J. Physiol. Heart Circ. Physiol.* **289,** H1456–H14567
45. Xiao, H. D., Fuchs, S., Campbell, D. J., Lewis, W., Dudley, S. C., Jr., Kasi, V. S., Hoit, B. D., Keshelava, G., Zhao, H., Capecchi, M. R., and Bernstein, K. E. (2004) *Am. J. Pathol.* **165,** 1019–1032
46. Severs, N. J., Bruce, A. F., Dupont, E., and Rothery, S. (2008) *Cardiovasc. Res.* **80,** 9–19
47. Witczak, C. A., Sharoff, C. G., and Goodyear, L. J. (2008) *Cell Mol. Life Sci.* **65,** 3737–3755
48. Chan, A. Y., and Dyck, J. R. (2005) *Can. J. Physiol. Pharmacol.* **83,** 24–28
49. Jørgensen, S. B., Viollet, B., Andreelli, F., Frosig, C., Birk, J. B., Schjerling, P., Vaulont, S., Richter, E. A., and Wojtaszewski, J. F. (2004) *J. Biol. Chem.* **279,** 1070–1079
50. Viollet, B., Andreelli, F., Jørgensen, S. B., Perrin, C., Geloen, A., Flamez, D., Mu, J., Lenzner, C., Baud, O., Bennoun, M., Gomas, E., Nicolas, G., Wojtaszewski, J. F., Kahn, A., Carling, D., Schuit, F. C., Birnbaum, M. J., Richter, E. A., Burcelin, R., and Vaulont, S. (2003) *J. Clin. Invest.* **111,** 91–98
51. Mu, J., Brozinick, J. T., Jr., Valladares, O., Bucan, M., and Birnbaum, M. J. (2001) *Mol. Cell* **7,** 1085–1094
52. Xing, Y., Musi, N., Fujii, N., Zou, L., Luptak, I., Hirshman, M. F., Goodyear, L. J., and Tian, R. (2003) *J. Biol. Chem.* **278,** 28372–28377
53. Zhang, P., Hu, X., Xu, X., Fassett, J., Zhu, G., Viollet, B., Xu, W., Wiczer, B., Bernlohr, D. A., Bache, R. J., and Chen, Y. (2008) *Hypertension* **52,** 918–924
54. Ouchi, N., Shibata, R., and Walsh, K. (2005) *Circ. Res.* **96,** 838–846